Litopenaeus vannamei stylicins are constitutively produced by hemocytes and intestinal cells and are differentially modulated upon infections

Natanael Dantas Farias, Marcelo Falchetti, Gabriel Machado Matos, Paulina Schmitt, Cairé Barreto, Nicolas Argenta, Jean-Luc Rolland, Evelyne Bachère, Luciane Maria Perazzolo, Rafael Diego Rosa

Litopenaeus vannamei stylicins are constitutively produced by hemocytes and intestinal cells and are differentially modulated upon infections

Natanael Dantas Farias [a,1], Marcelo Falchetti [a,1], Gabriel Machado Matos [a], Paulina Schmitt [b], Cairé Barreto [a], Nicolas Argenta [a], Jean-Luc Rolland [c], Evelyne Bachère [c], Luciane Maria Perazzolo [a], Rafael Diego Rosa [a,*]

a Laboratory of Immunology Applied to Aquaculture, Department of Cell Biology, Embryology and Genetics, Federal University of Santa Catarina, 88040-900, Florianópolis, SC, Brazil

b Laboratorio de Genética e Inmunología Molecular, Instituto de Biología, Facultad de Ciencias, Pontificia Universidad Católica de Valparaíso, 2373223, Valparaíso, Chile

c Interactions Hôtes-Pathogènes-Environnements, Université de Montpellier, CNRS, Ifremer, Université de Perpignan Via Domitia, 34090, Montpellier Cedex 5, France

∗ Corresponding author. E-mail address: rafael.d.rosa@ufsc.br (R.D. Rosa).

1 These authors contributed equally to this work.

ABSTRACT

Stylicins are anionic antimicrobial host defense peptides (AAMPs) composed of a proline-rich N-terminal region and a C-terminal portion containing 13 conserved cysteine residues. Here, we have increased our knowledge about these unexplored crustacean AAMPs by the characterization of novel stylicin members in the most cultivated penaeid shrimp, *Litopenaeus vannamei*. We showed that the *L. vannamei* stylicin family is composed of two members (*Lvan*-Stylicin1 and *Lvan*-Stylicin2) encoded by different loci which vary in gene copy number. Unlike the other three gene-encoded antimicrobial peptide families from penaeid shrimp, the expression of *Lvan*- Stylicins is not restricted to hemocytes. Indeed, they are also produced by the columnar epithelial cells lining the midgut and its anterior caecum. Interestingly, *Lvan*-Stylicins are simultaneously transcribed at different transcriptional levels in a single shrimp and are differentially modulated in hemocytes after infections. While the expression of both genes showed to be responsive to damage-associated molecular patterns, only *Lvan*-Stylicin2 was induced after a *Vibrio* infection. Besides, *Lvan*-Stylicins also showed a distinct pattern of gene expression in the three portions of the midgut (anterior, middle and posterior) and during shrimp development. We provide here the first evidence of the diversity of the stylicin antimicrobial peptide family in terms of sequence and gene expression distribution and regulation.

KEYWORDS

Crustacean - Penaeid shrimp - Invertebrate immunity - Antimicrobial peptide - Host defense peptide – Molecular diversity

1. Introduction

Antimicrobial host defense peptides (AMPs) are important components of the innate immune system of both vertebrates and invertebrates. They are usually described as gene-encoded peptides (less than 10 kDa) with cationic and amphipathic properties which selectively target the negatively charged membranes of microbes [1]. In addition to those classical cationic antimicrobial peptides (also known as CAMPs), the current classification of AMPs also includes polypeptides/proteins larger than 10 kDa, AMPs generated by the processing of precursor molecules and anionic peptides [2]. Anionic antimicrobial peptides (AAMPs) comprise a non-phylogenetic group of either geneencoded or non-ribosomally synthesized molecules with a high proportion of anionic amino acid residues (aspartate and glutamate). AAMPs are widely distributed in living organisms and play an important role in host defense against bacteria, fungi and viruses [3]. Like their cationic counterparts, AAMPs are multifunctional molecules engaged in different biological and immunological processes beyond antimicrobial functions [3].

Shrimp farming is an important economic activity for many developing countries in Asia and Latin America, which has been repeatedly threatened by infections caused by viruses and pathogenic bacteria from the genus *Vibrio*. Consequently, infectious disease outbreaks are clearly a major concern in aquaculture that has encouraged extensive research efforts. The scientific findings in the last decade have provided valuable information on the role of AMPs in shrimp defenses. More than natural antibiotics, shrimp AMPs are also involved in the control of the natural microbiota, wound healing, bacterial clearance and other immunomodulatory functions [4]. To date, four gene-encoded AMP families have been identified in the hemocytes of penaeid shrimp: penaeidins, crustins, anti-lipopolysaccharide factors (ALFs) and stylicins [4,5].

Stylicins were initially identified as transcripts associated to shrimp survival to pathogenic *Vibrio* infections [6]. Characterization of stylicins revealed that they are anionic peptides of 8.9 kDa composed of an Nterminal proline-rich region followed by a C-terminal region containing 13 cysteine residues [7]. In *Litopenaeus stylirostris* shrimp, stylicins form a diverse AAMP family composed of two members, named *Lsty*-Stylicin1 and *Lsty*-Stylicin2. Although the antimicrobial activity of the recombinant r*Lsty*-Stylicin1 has been shown to be restricted to filamentous fungi, the r*Lsty*-Stylicin1 displayed a strong lipopolysaccharide (LPS)-binding activity and the ability to agglutinate Gram-negative bacteria [7]. In the kuruma prawn *Marsupenaeus japonicus*, the gene expression of its single stylicin (*Mjap*-Stylicin) showed to be modulated in gills and hepatopancreas in response to the White spot syndrome virus (WSSV) [8]. Curiously, apart from these two reports [7,8], no other stylicin members have been characterized thus far.

In order to fill this research gap, novel members of the stylicin AMP family were identified and characterized in the most important cultured penaeid species, *Litopenaeus vannamei* (*Lvan*-Stylicin1 and *Lvan*- Stylicin2). We showed that *Lvan*-Stylicins (also known as *Vibrio penaeicida*-induced cysteine and proline-rich peptides or LvVICPs [9]) are highly anionic peptides encoded by two distinct genomic loci that follow different patterns of gene regulation during shrimp development and after microbial infections. Interestingly, while both genes responded to danger/damage-associated molecular patterns (shrimp muscle tissues), only *Lvan*-Stylicin2 showed to be up-regulated in circulating hemocytes in response to a *Vibrio* infection. Moreover, by combining immunohistochemistry and whole-mount immunofluorescence assays, we showed that *Lvan*-Stylicins are also constitutively produced by the midgut columnar epithelial cells. To our knowledge, this is the first evidence for the expression of a shrimp geneencoded AMP in other tissues than the immune cells from the hemolymph.

2. Materials and methods

2.1. Animals, immune challenge and tissue collection

Juvenile Pacific white shrimp (*Litopenaeus vannamei*) (10 ± 2 g) were obtained from the Laboratory of Marine Shrimp of the Federal University of Santa Catarina (Southern Brazil). After an acclimation period of seven days, animals (n=5) were stimulated by the injection of 5×107 colony-forming units (CFU)/animal of heat killed (70 °C for 20 min) *Vibrio harveyi* ATCC 14126 in 100 µL sterile seawater (SSW). Naïve (unchallenged) animals (n=5) were used as control. At 48 h post-stimulation, hemolymph was withdrawn into modified Alsever solution (MAS: 27mM sodium citrate, 336mM NaCl, 115mM glucose, 9mM EDTA, pH 7.0) and hemocytes were separated from plasma by centrifugation (800×g for 10 min at 4 °C). Shrimp were subsequently anesthetized (ice bath for 10 min) and sacrificed for the collection of the following tissues: gills, muscle, nerve cord, hepatopancreas, foregut, midgut and hindgut. Tissue samples were washed in Tris-saline solution (10mM Tris, 330mM NaCl, pH 7.4), homogenized in TRIzol reagent (Thermo Scientific) and immediately processed for total RNA isolation and tissue distribution analysis. Pleopods from naïve shrimp were collected and processed for genomic DNA (gDNA) extraction.

2.2. Experimental infections

Two unrelated shrimp pathogens were chosen for experimental infections, the Gram-negative *Vibrio harveyi* and the White spot syndrome virus (WSSV). For the bacterial infection, 6×107 CFU/animal of live V. *harveyi* ATCC 14126 in 100 µL SSW (median lethal dose within 2 days, LD50/2) or 100 µL SSW (injury control) were injected. For the viral infection, shrimp were injected with 100 µL of a WSSV inoculum containing 3×102 viral particles (median lethal dose within 15 days, LD50/15). The WSSV inoculum was prepared from muscle tissues of WSSV-infected shrimp as previously described [10]. Control animals for the viral infection were injected with 100 µL of a muscle tissue homogenate prepared from WSSV-free shrimp. At 48 h post-infections, circulating hemocytes and midguts were collected, pooled (3 pools of 5 animals per condition) and processed for total RNA extraction and quantitative PCR analysis of gene expression. Unchallenged animals (naïve shrimp at time 0 h) were used as control for all experiments.

In a second experiment, individual shrimp (n=3) were challenged by the oral administration of 7.5×105 CFU/animal of live V. *harveyi* ATCC 14126 in 50 µL SSW. Shrimp (n=3) that received SSW served as controls. The bacterial *per os* challenge was performed as previously described [11]. No mortalities were recorded during the course of the experiment. At 21 h post-challenge, midguts from both *Vibrio*-challenged and unchallenged shrimp were collected and flushed with cold Tris-saline solution and then cut into three equal portions (anterior, middle and posterior). Each individual sample was homogenized in TRIzol reagent (Thermo Scientific) and processed for total RNA extraction and quantitative PCR analysis of gene expression.

2.3. Genomic DNA and total RNA extraction and cDNA synthesis

For gDNA extraction, individual pleopods were homogenized and incubated at 55 °C for 1 h in 500 µL of lysis buffer (100mM Tris-HCl pH 8.5, 100mM NaCl, 50mM EDTA pH 8.0, 1% SDS, 0.25 µg/µL proteinase K). After addition of 3M potassium acetate (1:2; v:v), samples were incubated at 4 °C for 30 min and centrifuged at 14,000×g for 10 min. Following precipitation with isopropanol, gDNA samples were washed in 70% ethanol and treated with 50 µg/mL RNase A (Fermentas) at 37 °C for 30 min.

Quantification and quality of gDNA samples were assessed by spectrophotometry and 0.8% agarose gel electrophoresis,respectively.

Total RNA was extracted using TRIzol reagent (Thermo Scientific) according to the manufacturer's instructions. RNA samples were treated with DNase I (Thermo Scientific) at 37 °C for 15 min and precipitated with 0.3M sodium acetate (pH 5.2) and isopropanol (1:1; v:v). RNA amount and quality were assessed by spectrophotometric analysis and the integrity of total RNA was analyzed by 0.8% agarose gel electrophoresis. Following heat denaturation (70 °C for 5 min), reverse transcription was performed using 1 µg of purified total RNA with 50 ng/µL oligo(dT)12-18 in a 20-µL reaction volume containing the RevertAid Reverse Transcriptase (Thermo Scientific), according to the manufacturer's instructions.

2.4. Molecular cloning

PCR amplifications for molecular cloning were conducted using primers based on the nucleotide sequence of two stylicin homologues (contigs: DN31608_c0_g1_i1 and DN31608_c0_g1_i2) identified in midgut transcriptomes of *L. vannamei* (unpublished data). PCR reactions were carried out in a 15-µL reaction volume containing 50–100 ng of gDNA, 2mM MgCl2, 0.4mM dNTP Mix, 0.4 µM of each primer (Table 1) and 1 U Taq DNA Polymerase (Sinapse). PCR conditions were as follows: 1 cycle of denaturation at 95 °C for 10 min followed by 35 cycles of 95 °C for 45 s, 55 °C for 45 s and 72 °C for 2 min, and a final extension step of 72 °C for 10 min. The amplification products were analyzed by electrophoresis (1.5% agarose gel) and cloned into a pCR2.1-TOPO vector (Thermo Scientific). The positive clones were identified by colony PCR and plasmid sequencing.

2.5. Sequence data analysis and phylogeny

Stylicin sequences from the penaeid species *L. vannamei* (contigs: DN31608_c0_g1_i1 and DN31608_c0_g1_i2), *L. stylirostris* (*Lsty*- Stylicin1: EU177435; *Lsty*-Stylicin2: EU177437) and *M. japonicus* (*Mjap*-Stylicin: KR063277) were used for the search of homologous sequences in the following publicly accessible databases: Expressed Sequence Tags (EST), Transcriptome Shotgun Assembly (TSA) and Whole-Genome Shotgun Contigs (WGS). Only full-length coding sequences were included. Homology searches were performed using tBLASTX at the NCBI web servers (http://www.ncbi.nlm.nih.gov/BLAST). All nucleotide sequences were manually inspected and translated using the ExPASy Translate Tool (http://web.expasy.org/translate/). Prediction of signal peptide was performed with the SignalP 4.1 program (http://www.cbs.dtu.dk/services/SignalP/) and the theoretical isoelectric point (p*I*) and molecular weight (MW) of the mature peptides were predicted using the ExPASy ProtParam Tool (http://web.expasy.org/protparam/). Phylogenetic analysis based on both nucleotide and predicted amino acid sequences were conducted in MEGA X [12] using the Maximum Likelihood method. Bootstrap sampling was reiterated 1000 times using a 50% bootstrap cutoff.

2.6. Semiquantitative RT-PCR analysis

The extraction of total RNA and cDNA synthesis were performed using the method described above. PCR reactions were carried out in a 15-µL reaction volume containing 1 µL of cDNA, 2mM MgCl2, 0.4mM dNTP Mix, 0.4 µM of each primer (Table 1) and 1 U Taq DNA Polymerase (Sinapse). PCR conditions were as follows: 1 cycle of denaturation at 95 °C for 5 min followed by 30 cycles of 95 °C for 30 s, 57 °C for 30 s and 72 °C for 30 s, and a final extension step of 72 °C for 10 min. PCR products were analyzed by electrophoresis (1.5% agarose gel) and stained by ethidium bromide. The expression of

the LvActin gene (PCR conditions: 40 cycles of 95 °C for 45 s, 50 °C for 45 s and 72 °C for 1 min) was used as endogenous control to normalize the RT-PCR data for comparison.

2.7. Immunodetection of stylicins in shrimp tissues

Whole juvenile shrimp (n=3) were fixed in Davidson's fixative solution (22% formalin, 31.5% ethanol and 11.5% glacial acetic acid) for 24 h at room temperature, embedded in paraffin and cut into 5 µm thick sections. Histological sections of shrimp tissues were deparaffinized and hydrated through xylene-ethanol-water series, and washed in Tris-buffered saline (TBS: 50mM Tris-HCl, 200mM NaCl, pH 7.2). Then, sections were permeabilized (1×TBS, 0.1% Triton X-100) for 30 min and blocked in TBS-T solution (1×TBS, 1% BSA, 0.05% Tween 20) for 2 h followed by 16 h incubation at 4 °C with mouse anti-r*Lsty*- Stylicin1 polyclonal antibodies (2.3 µg/mL) [7]. After three washes in 1 × TBS+0.05% Tween 20 buffer, sections were incubated for 3 h at room temperature with alkaline phosphatase-labeled rabbit antimouse IgG (1:1000) (Thermo Scientific), followed by a 1 h incubation at room temperature in the dark in a solution of 100 mM Tris-HCl, 100 mM NaCl, 50 mM MgCl2 (pH 9.3) containing 0.175 mg/mL 5- bromo-4-chloro-3-indolyl phosphate (BCIP) (Sigma), 0.375 mg/mL nitro blue tetrazolium (NBT) (Sigma) and 0.24 mg/mL levamisole (Sigma). Negative controls consisted in replacing anti-r*Lsty*-Stylicin1 antibodies with pre-immune mouse serum or TBS-T solution.

Whole-mount immunofluorescence assays were conducted in midgut samples from juvenile shrimp (n=3). Midguts were harvested by dissection, washed in ice-cold Tris-saline solution and immediately fixed in 4% paraformaldehyde. Just after removal of the intestinal content, midguts were longitudinally opened, washed in phosphatebuffered saline (PBS: 137mM NaCl, 2.7mM KCl, 10mM Na2HPO4, 2mM KH2PO4, pH 7.2) and blocked in PBS-T solution (1×PBS, 1% BSA, 0.1% Triton X-100) for 3 h followed by 16 h incubation at 4 °C with mouse anti-r*Lsty*-Stylicin1 polyclonal antibodies (2.3 µg/mL) [7]. Midguts were then washed 3 times with PBS-T solution for 20 min and Incubated for 4 h at room temperature with 4',6-diamidino-2-phenylindole (DAPI) and FITC-conjugated anti-mouse secondary antibodies diluted at 1:500 (Thermo Scientific). Negative controls consisted in replacing the primary antibodies with pre-immune mouse serum or PBS-T solution. The experiments were repeated three times, and representative images were taken by confocal microscope (Leica DMI6000 B Microscope).

2.8. Fluorescence-based reverse transcription real-time quantitative PCR (RT-qPCR)

RT-qPCR reactions were performed in a final volume of 15 µL containing 0.2 µM of each primer (Table 1), 7.5 µL of Maxima SYBR Green/ ROX qPCR Master Mix (Thermo Scientific) and 1 µL of cDNA. The RTqPCR program was 95 °C for 10 min, followed by 40 cycles of 95 °C for 15 s and 60 °C for 60 s. Melt curve analysis (60–95 °C at a temperature transition rate of 0.05 °C/s) was performed to evaluate primer specificity. Primer pair efficiencies (E) were calculated from 2-fold dilution series of pooled cDNA for each primer pair. Primer pair efficiencies were calculated from the given slopes in the StepOne software v2.3, according to the equation: E=10(−1/slope).

The eukaryotic translation elongation factor 1-alpha (*Lv*EF1α) and the ribosomal proteins LvL40, *Lv*RpS3A and *Lv*RpS6 (Table 1) were used as reference genes of expression data in circulating hemocytes. In midgut, *Lv*EF1α, *Lv*L40 and *Lv*Actin were used as reference genes for data normalization [13]. The relative expression levels of *Lvan*-Stylicins were calibrated with the expression profile of circulating hemocytes or midguts from naïve (unchallenged) shrimp, according to the 2−ΔΔCq method [14]. Differences in gene expression were considered statistically significant at $P < 0.05$ (cutoff of 1.5-fold change in expression levels) using one-way ANOVA and Tukey's multiple comparison test.

The transcript abundance of *Lvan*-Stylicins in three midgut portions (anterior, middle and posterior) from *Vibrio*-challenged and naïve (unchallenged) shrimp was quantified by RT-qPCR and normalized with the gene expression of *Lv*EF1α, *Lv*RpS3A, *Lv*RpS6 and *Lv*Actin (Table 1). The relative expression levels were calibrated with the gene expression of each midgut portion from unchallenged shrimp and differences were considered statistically significant at $P < 0.05$ (cutoff of 1.5-fold change in expression levels) using Student's t-test.

2.9. Gene copy number estimation and basal mRNA levels

The number of *Lvan*-STY gene copies in *L. vannamei* genome was estimated in five individual shrimp by absolute quantification through the qPCR technique. qPCR reactions were performed using specific primers (Table 1) and 80 ng of gDNA as template. The absolute quantification of the target genes (*Lvan-STY1* and *Lvan-STY2*) was calculated using a standard curve derived from 10-fold dilution series of plasmids containing the DNA target sequences (107 to 103 plasmids/µL; R2=0.998 and 0.999 for *Lvan-STY1* and *Lvan-STY2*, respectively). The transcript abundance of *Lvan*-Stylicin1 and *Lvan*-Stylicin2 in the circulating hemocytes of the same five shrimp individuals was assessed by absolute quantification using 1 ng of reverse-transcribed total RNA. The absolute mRNA quantification was performed using the same method described for the gene copy number estimation.

The comparison of the transcript abundance of *Lvan*-Stylicins between hemocytes and midgut was assessed by RT-qPCR (3 pools of 4 animals per tissue) and normalized with the gene expression of *Lv*EF1α, *Lv*RpS3A and *Lv*RpS6 (Table 1), according to the $2^{-\Delta\Delta Cq}$ method [14]. Differences in gene expression between tissues were considered statistically significant at $P < 0.05$ (cutoff of 1.5-fold change in expression levels) using Student's t-test.

2.10. Quantitative gene expression analysis during shrimp development

Three biological replicates of different development stages of *L. vannamei* were collected: fertilized eggs at 0–4 h (EI) and at 7–11 h postspawning (EII), nauplius I and V (NI and NV), protozoea I and III (ZI and ZIII), mysis I and III (MI and MIII) and postlarvae aged of 2, 9 and 17 days (PL2, PL9 and PL17). Transcript levels of *L. vannamei* stylicins during shrimp development were quantified by RT-qPCR and normalized with the gene expression of *Lv*RpS6 and *Lv*Actin (Table 1), as previously described [15]. Hemocyte samples from juveniles (3 pools of 5 animals) were used as control for calibrating gene expression data. Genes were considered as “not expressed” in a specific development stage when PCR amplification yielded no product (no dissociation curves) whereas RT-qPCR reactions showing Cq values higher than the limit of quantification (but that generated an expected dissociation curve profile) were considered as “unquantifiable”. Statistical significance was considered at $P < 0.05$ by one-way ANOVA followed by Tukey's multiple comparison test.

3. Results

3.1. L. vannamei stylicins comprise a diverse AAMP family

The transcriptomic analysis of the *L. vannamei* midgut (unpublished) has revealed the presence of two nucleotide sequences (contigs: DN31608_c0_g1_i1 and DN31608_c0_g1_i2) homologous to the stylicin antimicrobial peptides from the blue shrimp *L. stylirostris* (*Lsty*-Stylicin1 and *Lsty*-Stylicin2). Both sequences correspond to full-length transcripts that encode for precursors composed of a signal peptide followed by a mature peptide containing 13 cysteine residues. The full-length stylicin sequences from *L. vannamei* were cloned by PCR amplification from gDNA samples and re-sequenced

for confirmation. The nucleotide sequence corresponding to the contig DN31608_c0_g1_i2 shared 86% identity with *Lsty*-Stylicin1 (GenBank: EU177435) whereas the contig DN31608_c0_g1_i1 shared 93% identity with *Lsty*-Stylicin2 (GenBank: EU177437). Thus, those sequences from *L. vannamei* were designated as *Lvan*-Stylicin1 (GenBank: MH108957) and *Lvan*-Stylicin2 (GenBank: MH108958), respectively (Fig. 1A).

The deduced amino acid sequences of *Lvan*-Stylicins start with a predicted 22-residue signal peptide followed by an anionic mature peptide of 82 amino acid residues (Fig. 1A; Table S1). Although *Lvan*- Stylicins contain no obvious protein domains, both mature peptides are characterized by the presence of a proline-rich N-terminal region and a C-terminal region holding the 13 conserved cysteine residues found in *L. stylirostris* stylicins and in the *Mjap*-Stylicin from *M. japonicus*. *Lvan*- Stylicins were quite similar to each other and to stylicins from *L. stylirostris* (> 80% identity), but less than 65% amino acid identity was observed between *Lvan*-Stylicins and *Mjap*-Stylicin.

In silico analysis of *L. vannamei* non-annotated databases publicly available on GenBank led to the identification of different isoforms for each *L. vannamei* stylicin: five for *Lvan*-Stylicin1 (GenBank: FE179060, FE156583, FE124653, FE125173 and GETD01027084) and three for *Lvan*-Stylicin2 (GenBank: GETD01027083, GETZ01053100 and GFRP01011277). Those sequences were identified in EST and TSA libraries from multiple shrimp tissues, such as hemocytes, lymphoid organ, nerve cord and hepatopancreas. Additionally, we included in this analysis the *Vibrio penaeicida*-induced cysteine and proline-rich peptides (*Lv*VICP1 and *Lv*VICP2), stylicin homologues identified in *L. vannamei* by Wang and colleagues [9]. While *Lvan*-Stylicin2 sequences differed only by synonymous and non-synonymous substitutions, *Lvan*- Stylicin1 sequences showed two distinct lengths: 82 or 83 amino acid residues (Fig. 1B; Table S1). Besides from the synonymous and nonsynonymous substitutions, *Lvan*-Stylicin1 peptides can be distinguished from each other by the presence/absence of a tyrosine (Y) or histidine (H) residue at the position 51 of the precursor peptide (Fig. 1B). The 82- residue *Lvan*-Stylicin1 peptides showed a molecular weight of 8.83 kDa and a calculated pI of 4.98 while the 83-residue *Lvan*-Stylicin1 peptides showed a molecular weight ranging from 8.97 to 9.02 kDa and a calculated pI of 4.98 or 5.19 (Table S1). Comparatively, the mature *Lvan*- Stylicin2 peptides had a molecular weight of about 9 kDa and a calculated pI ranging from 4.47 to 4.69 (Table S1).

3.2. L. vannamei stylicins are encoded by distinct genomic loci

The genomic organization of *L. vannamei* stylicin genes (*Lvan-STY1* and *Lvan-STY2*) was investigated in two individual shrimp using PCRbased and cloning strategies. Sanger DNA sequencing results showed that *Lvan*-Stylicins are encoded by distinct genomic sequences, but share a similar structural gene organization (Fig. 2A). *Lvan-STY1* and *Lvan-STY2* genes are composed by two exons interrupted by a single intron with a length of 217 bp and 205 bp, respectively (Fig. 2A). Both genomic DNA sequences followed the canonical GT/AG splicing recognition rule at the exon/intron boundaries (Fig. S1). In both genes, the first exon covers the 5'-untranslated region (UTR), the signal peptide and the first three residues of the mature peptide while the second exon encodes the remainder of the mature peptide sequence and the 3'- UTR.

Interestingly, the *Lvan-STY1* genes from the two sampled shrimp were identical to each other while the nucleotide sequence of their *Lvan-STY2* genes differed in ten nucleotides: one in the first exon, five in the intron and four in the second exon (Fig. S1). The five nucleotide substitutions found in the coding sequence resulted in the change of two amino acid residues. The obtained genomic sequences were deposited in GenBank under the accession numbers MH108959 to MH108962.

Then, we asked whether *Lvan-STY1* and *Lvan-STY2* genes have the same number of copies in *L. vannamei* genome. The relative gene copy number ratio of *Lvan-STY2*/*Lvan-STY1* was estimated in five individual animals by quantitative PCR. The number of *Lvan-STY2* gene copies was 2.37 ± 0.15-fold higher than the number of copies of the *Lvan-STY1* gene (Fig. 2B). Finally, a phylogenetic analysis showed that the *Lvan-* STY genes were placed in the same clade with the stylicin genes from *L. stylirostris* (*Lsty-STY1*: EU177436 and *Lsty-STY2*: EU177437) (Fig. 2C). In this clade, *Lvan-STY1* and *Lsty-STY1* clustered together in a single group distinct to the *STY2* genes (Fig. 2C). Stylicin genes from *P. monodon* (*Pmon-STY*: NIUS012084699) and *M. japonicus* (*Mjap*-STY: NIUR011088360) clustered in separate groups.

3.3. Stylicins cluster into three distinct phylogenetic groups

In silico mining of publicly accessible databases (EST, TSA and WGS) resulted in the identification of novel members of the Stylicin family in different penaeid species: *Fenneropenaeus penicillatus* (*Fpen*-Stylicin: GFRT01005742), *M. japonicus* (*Mjap*-Stylicin: NIUR011088360) and *P. monodon* (*Pmon-STY*licin: JZ892895, DW678047, DW678039, DT366712, DW042940, GW996588, GEEP01015864, GEME01013089 and NIUS012084699). From our *In silico* analysis, stylicin sequences were only identified in penaeid shrimp species. All obtained sequences hold the 13 conserved cysteine residues at the C-terminal region (Fig. 3A).

Phylogenetic analysis revealed that the Stylicin family is a monophyletic group that evo*Lv*ed from a common ancestor gene. Phylogenetic trees constructed with nucleotide and predicted amino acid sequences shared similar topological structures. As shown in Fig. 3B, stylicins clustered in three main clades. The first clade included only stylicin sequences from penaeid species from the genus Litopenaeus. In this clade, Stylicin1 and Stylicin2 were split into two distinct groups (Fig. 3B). Finally, while *Pmon-STY*licins and Fpen-Stylicin clustered in a second phylogenetic group, *Mjap*-Stylicins formed a separate clade from all stylicin sequences (Fig. 3B).

3.4. Stylicins are constitutively produced by hemocytes and intestinal cells

The gene expression distribution of *L. vannamei* stylicins was first evaluated in eight different tissues of shrimp stimulated or not by the injection of heat-killed V. *harveyi*. Results from the semiquantitative RTPCR analysis evidenced the presence of *Lvan*-Stylicin1 transcripts in circulating hemocytes, foregut, midgut and gills (Fig. 4). In *Vibrio*-stimulated animals, *Lvan*-Stylicin1 gene expression was also detected in hindgut and nerve cord. Comparatively, transcripts of *Lvan*-Stylicin2 were detected in circulating hemocytes, foregut, midgut, hindgut, gills and nerve cord of both stimulated and non-stimulated animals (Fig. 4). For both *Lvan*-Stylicins, no signals were observed in muscle and hepatopancreas (Fig. 4).

To characterize the peptide localization of *Lvan*-Stylicins, immunohistochemistry analysis was subsequently performed on sections of different shrimp tissues using polyclonal antibodies raised against the r*Lsty*-Stylicin1 from *L. stylirostris* [7]. Due to the high degree of sequence conservation, anti-*Lsty*-Stylicin1 antibodies probably recognized both *Lvan*-Stylicins. Stylicin immunoreactivity was found in individual cells heterogeneously distributed across the shrimp tissues. In the cephalothorax, positive immunoreactivity was especially pronounced in some cells present in the connective tissue of the anterior midgut caecum (Fig. 5A and B). Based on morphological features, those stylicin-positive cells are likely tissue-infiltrating hemocytes.

Besides those cells, stylicin immunoreactivity was also observed in the apical region of the columnar epithelial cells lining the midgut and its anterior caecum (Fig. 5A and B). Whole-mount

immunofluorescence assays were further performed to confirm the presence of stylicin peptides in those epithelial cells. Confocal images clearly evidenced the presence of stylicin-containing granules located at the apical region of the midgut columnar epithelial cells (Fig. 5C–E). No signals were observed in other cell types of the shrimp body, thus the results of the semiquantitative RT-PCR analysis are probably the consequence of the infiltration of stylicin-expressing hemocytes in shrimp tissues. Altogether, results from both immunohistochemistry and whole-mount immunofluorescence assays showed that *Lvan*-Stylicins are constitutively produced by the hemocytes and by the columnar epithelial cells of the midgut.

3.5. Lvan-STY1 and Lvan-STY2 genes are simultaneously transcribed in a single shrimp at different basal levels

Since *Lvan*-Stylicins are produced by both hemocytes and midgut cells, we focused on determining the main site of stylicin expression in penaeid shrimp. Results showed that the expression of *Lvan*-Stylicin1 and *Lvan*-Stylicin2 was, respectively, 52.5-fold and 62.2-fold higher in circulating hemocytes than in the midgut (Fig. 6A). Next, the basal mRNA expression levels of the *Lvan-STY1* and *Lvan-STY2* genes were analyzed in the circulating hemocytes of five individual shrimp by absolute quantification. Interestingly, both *Lvan*-STY genes showed to be constitutively and simultaneously transcribed in an individual shrimp, but at different transcriptional levels. The basal expression of *Lvan-STY2* was 3.69-fold higher than *Lvan-STY1* (Fig. 6B). Besides, the basal mRNA levels of each gene showed to be also variable among the individuals (Fig. 6B). For the *Lvan-STY1* gene, differences in gene expression reached up to 3.78-fold whereas variations up to 2.36-fold were found in *Lvan-STY2* gene expression.

3.6. The gene expression of L. vannamei stylicins is differentially modulated in response to infections

The gene expression profile of *Lvan*-Stylicins was further quantified by fluorescence-based quantitative PCR (RT-qPCR) in shrimp hemocytes and midgut at 48 h after infections with two unrelated pathogens, the Gram-negative V. *harveyi* and the WSSV. This time point was chosen on the basis of previous studies from our group [10,13]. Interestingly, while the expression of *Lvan*-Stylicin2 was induced in circulating hemocytes in response to the *Vibrio* infection (2.4-fold change), the expression of *Lvan*-Stylicin1 was not modulated (Fig. 7). No increase in *Lvan*-Stylicin2 expression was observed following the injection of sterile seawater (aseptic injury control). Besides, both genes were not modulated after the viral infection. In contrast, the expression of both genes was up-regulated in circulating hemocytes (2.5-fold change for *Lvan*-Stylicin1 and 2.9-fold change for *Lvan*-Stylicin2) after the injection of a muscle tissue homogenate prepared from WSSV-free shrimp (Fig. 7). In the midgut, the expression of *Lvan*-Stylicins was not regulated by the bacterial or by the viral infection (Fig. 7).

The lack of gene expression response in the midgut encouraged us to conduct an alternative experimental infection method, mimicking a more natural route of bacterial infection (*per os* challenge). Variations in gene expression of *Lvan*-Stylicins were assessed by RT-qPCR in three midgut portions (anterior, middle and posterior). The expression of both *Lvan*-Stylicins was up-regulated (2.89-fold change for *Lvan*- Stylicin1 and 4.31-fold change for *Lvan*-Stylicin2) only in posterior portion of the midgut (Fig. 8). By contrast, no increase in *Lvan*-Stylicin gene expression was observed in the two first midgut portions (anterior and middle) in response to the oral *Vibrio* challenge (Fig. 8).

3.7. L. vannamei stylicins show a different pattern of gene expression during shrimp development

We finally investigated the presence and the levels of stylicin transcripts in twe*Lv*e developmental stages of *L. vannamei*, from fertilized eggs to larval (nauplius, protozoea and mysis) and postlarval stages, and also in circulating hemocytes from juveniles. Transcript levels of *Lvan*-Stylicin1 were detected at very low levels in late protozoea stages (ZIII), but its expression was only quantified from mysis III (MIII). Then, *Lvan*-Stylicin1 expression increased gradually in the following developmental stages (Fig. 9). On the other hand, *Lvan*-Stylicin2 transcripts were found to be present early in shrimp development (fertilized eggs at 7–11 h post-spawning). However, *Lvan*-Stylicin2 expression was only quantified from the protozoea III (ZIII) stage (Fig. 9). For both genes, the highest mRNA abundance was quantified in hemocytes from juvenile shrimp (Fig. 9).

4. Discussion

We showed here that *L. vannamei* stylicins comprise a diverse family of anionic antimicrobial peptides (AAMPs) whose genes are differentially regulated in hemocytes and midgut cells in response to infections. From the four gene-encoded AMPs described in penaeid shrimp, only stylicins have not been fully characterized in the Pacific white shrimp (*L. vannamei*) and this is the first study exploring the diversity of the stylicin family in terms of sequence and gene expression distribution and regulation. By taking advantage of RNA-Seq technology, we have identified two stylicin homologues (*Lvan*-Stylicin1 and *Lvan*-Stylicin2) in midgut transcriptomes of *L. vannamei* showing high similarities to stylicins from the blue shrimp *L. stylirostris* [7]. From our *In silico* analysis, stylicins form a diverse gene family in shrimp species of the genus Litopenaeus, but not in other taxa of the family Penaeidae, such as Fenneropenaeus, Penaeus and Marsupenaeus. Essentially, our results revealed that all known Litopenaeus gene-encoded AMPs are present as diverse multigene families composed of different members. For instance, while Litopenaeus penaeidins are composed of three members (*Litvan* PEN1/2, *Litvan* PEN3 and *Litvan* PEN4), at least four and seven members were identified in the crustin (Crustin *Lv*, Crustin-like *Lv*, *Lv*SWD and *Lv*SPLI) and in the ALF families (*Litvan* ALF-A to -G), respectively [4,5,16]. However, unlike other gene-encoded AMPs from marine invertebrates, stylicins are exclusively composed of anionic peptides. Interestingly, the spectrum of activity of these anionic antimicrobials is restricted to filamentous fungi [7], even if their gene expression has shown to be associated to shrimp survival to pathogenic *Vibrio* infections [6]. Likewise, anionic peptides derived from the Cterminus of the shrimp respiratory protein hemocyanin are also specific against fungi [17]. These hemocyanin-derived peptides, named PvHCt, are able to bind and permeabilize fungal membranes [18]. To date, the mechanism of action of stylicins and of other AAMPs is completely unknown. Actually, in comparison to CAMPs, few scientific groups have attempted to study the subject of AAMPs [3] and more functional studies are needed to achieve a more in-depth understanding of these unconventional AMPs.

We showed here that *Lvan*-Stylicin1 and *Lvan*-Stylicin2 are encoded by different genomic loci. Nonetheless, the presence of distinct stylicin genes was only observed in Litopenaeus species. Thus, it is likely that *STY1* and *STY2* are paralogous genes that arose from a single gene duplication event before the speciation of the genus Litopenaeus. Besides, although both *Lvan*-STY genes share a similar structural gene organization, their copy numbers in *L. vannamei* genome showed to be variable, suggesting that they have followed independent duplication events after *STY1-STY2* divergence. Apart from the two main stylicins members (*Lvan*-Stylicin1 and *Lvan*-Stylicin2), we have identified *Lvan*-

Stylicin1 sequences with distinct lengths (82 and 83 amino acids in length). No evidences for the presence of alternative splicing were found in the *Lvan-STY1* gene, and thus it is most likely that different alleles may occur for *L. vannamei* stylicin genes. Taken together, our results suggest that *L. vannamei* stylicins belong to a diverse multigenic and multiallelic family of AAMPs. Moreover, *Lvan-STY1* and *Lvan-STY2* genes showed to be simultaneously transcribed in a single shrimp. The different penaeidin and ALF members are also simultaneously expressed in an individual shrimp [16,19], and it would be of great interest to colocalize the four gene-encoded AMP families in shrimp hemocytes and examine whether they function synergistically to enhance their antimicrobial spectrum of activity. Synergic activities have already been observed for AMPs from both vertebrate [20] and invertebrate species [21,22], but unfortunately, no studies of this type have been addressed in crustaceans.

One of the most important findings of this study is that the expression *Lvan*-Stylicins is not limited to the immune cells (hemocytes) as observed for the other three shrimp gene-encoded AMPs [4]. Both immunostaining and gene expression analysis revealed that *Lvan*-Stylicins are constitutively produced by the midgut columnar epithelial cells and that their expression is induced in response to *Vibrio* infections. Notably, the expression of *Lvan*-Stylicin was pronounced in the anterior midgut caecum, an intestinal region primarily invo*Lv*ed in the production, secretion and activation of digestive enzymes [23]. Thus, it is plausive to hypothesize that *Lvan*-Stylicins are secreted into the midgut lumen. This finding brings new insights into the role of crustacean AMPs in the control of the gut microbiota and in shrimp intestinal defenses. Indeed, the shrimp midgut lacks the cuticular lining found in the other portions of the intestine (foregut and hindgut), representing a potential route of entry for many pathogens into the hemocel. In a previous study, we showed that gut is an important source for the expression of immune-related genes in penaeid shrimp [13], thus the presence of stylicins in the midgut cells suggests the participation of these antimicrobial effectors in the first intestinal line of defense. Interestingly, the expression of some ALF members showed to be invo*Lv*ed in the maintenance of the microbiota residing in the shrimp hemolymph [24]. Taken all together, our results highlight the importance of stylicins in both hemolymph-based and gut-based immunities.

Another relevant conclusion that can be drawn from this study is that *Lvan*-STY genes are differentially regulated after infections. Such diversity in gene expression regulation was previously reported for the different members of the *L. vannamei* ALF family in response to fungal infections [25]. Interestingly, while some AMPs such as *Lvan*-Stylicin1, penaeidins [26], *Litvan* ALF-A [25] and Type II crustins [27] are notregulated in response to infections, the expression of other *L. vannamei* AMPs (*Lvan*-Stylicin2 and other ALF members) is induced in immune cells to improve host antimicrobial responses against pathogens. As elegantly shown by Wang et al. [9], the gene expression of most shrimp AMPs, including penaeidins, Type II crustins and stylicins (*Lv*VICPs), is controlled by the IMD/NF-κB pathway, an evolutionarily conserved signaling cascade invo*Lv*ed in the regulation of the antimicrobial responses of arthropods. On the other hand, the expression of almost all shrimp AMPs, including *Lvan*-Stylicins, can be drastically affected in circulating hemocytes during lethal infections [10]. Unlike the *Mjap*- Stylicin from the kuruma prawn *M. japonicus* [8], *Lvan*-Stylicins were not modulated neither in circulating hemocytes nor in midgut by the WSSV. This result could be probably due to the time course response of *Lvan*-Stylicins in those shrimp tissues. On the other hand, both *Lvan*-STY genes have been shown to be responsive to a tissue homogenate prepared from shrimp muscle (injury control for the WSSV infection). This finding strongly suggests that *Lvan*-Stylicins are induced in response to danger/damage-associated molecular patterns (DAMPs) and that these AAMPs could be invo*Lv*ed in early inflammation and in wound healing processes as proposed for penaeidins [26].

L. vannamei stylicin genes showed to be differentially regulated not only in response to infections, but also during shrimp development. Interestingly, *Lvan*-Stylicin2 and the *M. japonicus* stylicin showed a very similar pattern of gene expression during shrimp development [8]. Comparatively, *Lvan*-Stylicin1 expression was quite similar to that observed for other *L. vannamei* AMPs, such as *Litvan* PEN1/2, *Litvan* PEN4 and *Litvan* ALF-D [15]. Apart from that, we cannot discard the possibility of these changes in gene expression could be the result of the differences in the mRNA basal levels observed between the *Lvan*-STY genes. Indeed, the detection of stylicin transcripts, as well as of other gene-encoded AMPs, highlights the importance of these antimicrobial effectors during shrimp development.

5. Conclusions

In conclusion, we showed that the stylicin family from shrimp species of the genus Litopenaeus is composed of two members encoded by distinct genomic loci that exhibit different patterns of gene expression distribution and regulation. According to the best of our knowledge, this is the first evidence for the expression of a shrimp gene-encoded AMP in other tissues than the hemocytes. Even though the expression of stylicins has been shown to be a marker of shrimp survival to pathogenic *Vibrio* infections, the role of these effectors in shrimp immune defense is still largely unknown. The application of RNAibased methods could make significant contributions to understanding the significance of the molecular and transcriptional diversity of Litopenaeus stylicins in host-microbe interactions.

Acknowledgments

We are grateful to the Laboratory of Marine Shrimp (Federal University of Santa Catarina - UFSC) for providing the shrimp used in this study and to Fabio S Ribeiro for his technical assistance in the whole-mount immunofluorescence experiments. The authors are also thankful to the Electronic Microscopy Central Laboratory (LCME-UFSC) and the Multiuser Laboratory of Biology Studies (LAMEB-UFSC). This work was supported by the Brazilian funding agencies CNPq (MEC/MCTI/CAPES/CNPq/FAPs PVE 401191/2014-1 and MCTI/CNPq Universal 406530/2016-5) and CAPES (CIMAR 1974/2014). P Schmitt was funded by FONDECYT grant 11150009. ND Farias and GM Matos were supported by scholarships provided by FAPESC while N Argenta received a scholarship provided by CNPq. M Falchetti and C Barreto were supported by fellowships provided by CAPES.

References

[1] K.A. Brogden, Antimicrobial peptides: pore formers or metabolic inhibitors in bacteria? Nat. Rev. Microbiol. 3 (2005) 238–250, https://doi.org/10.1038/nrmicro1098.

[2] N.Y. Yount, A.S. Bayer, Y.Q. Xiong, M.R. Yeaman, Advances in antimicrobial peptide immunobiology, Biopolymers 84 (2006) 435–458, https://doi.org/10.1002/bip.20543.

[3] F. Harris, S. Dennison, D. Phoenix, Anionic antimicrobial peptides from eukaryotic organisms, Curr. Protein Pept. Sci. 10 (2009) 585–606, https://doi.org/10.2174/138920309789630589.

[4] D. Destoumieux-Garzón, R.D. Rosa, P. Schmitt, C. Barreto, J. Vidal-Dupiol, G. Mitta, et al., Antimicrobial peptides in marine invertebrate health and disease, Philos Trans R Soc B Biol Sci 371 (2016) 20150300, https://doi.org/10.1098/rstb.2015.0300.

[5] R.D. Rosa, M.A. Barracco, Antimicrobial peptides in crustaceans, Invertebr. Surviv. J. 7 (2010) 262–284.

[6] J. de Lorgeril, D. Saulnier, M.G. Janech, Y. Gueguen, E. Bachère, Identification of genes that are differentially expressed in hemocytes of the Pacific blue shrimp (*Litopenaeus stylirostris*) surviving an infection with *Vibrio penaeicida*, Physiol.Genom. 21 (2005) 174–183, https://doi.org/10.1152/physiolgenomics.00281.2004.

[7] J.L. Rolland, M. Abdelouahab, J. Dupont, F. Lefevre, E. Bachère, B. Romestand, Stylicins, a new family of antimicrobial peptides from the Pacific blue shrimp *Litopenaeus stylirostris*, Mol. Immunol. 47 (2010) 1269–1277, https://doi.org/10.1016/j.molimm.2009.12.007.

[8] H. Liu, J. Wang, Y. Mao, M. Liu, S. Niu, Y. Qiao, et al., Identification and expression analysis of a novel stylicin antimicrobial peptide from Kuruma shrimp (*Marsupenaeus japonicus*), Fish Shellfish Immmunology 47 (2015) 817–823, https://doi.org/10.1016/j.fsi.2015.09.044.

[9] P.H. Wang, D.H. Wan, Z.H. Gu, W. Qiu, Y.G. Chen, S.P. Weng, et al., Analysis of expression, cellular localization, and function of three inhibitors of apoptosis (IAPs) from *Litopenaeus vannamei* during WSSV infection and in regulation of antimicrobial peptide genes (AMPs), PLoS One 8 (2013) e72592, , https://doi.org/10.1371/journal.pone.0072592.

[10] P. Gonca*Lv*es, C. Guertler, E. Bachère, C.R.B. de Souza, R.D. Rosa, L.M. Perazzolo, Molecular signatures at imminent death: hemocyte gene expression profiling of shrimp succumbing to viral and fungal infections, Dev. Comp. Immunol. 42 (2014) 294–301, https://doi.org/10.1016/j.dci.2013.09.017.

[11] M. Pilotto, A. Gonca*Lv*es, F. Vieira, W. Seifert, E. Bachère, R.D. Rosa, et al., Exploring the impact of the biofloc rearing system and an oral WSSV challenge on the intestinal bacteriome of *Litopenaeus vannamei*, Microorganisms 6 (2018) 83, https://doi.org/10.3390/microorganisms6030083.

[12] S. Kumar, G. Stecher, M. Li, C. Knyaz, K. Tamura, MEGA X: molecular evolutionary genetics analysis across computing platforms, Mol. Biol. Evol. 35 (2018) 1547–1549, https://doi.org/10.1093/molbev/msy096.

[13] A.S. Si*Lv*eira, G.M. Matos, M. Falchetti, F.S. Ribeiro, A. Bressan, E. Bachère, et al., An immune-related gene expression atlas of the shrimp digestive system in response to two major pathogens brings insights into the invo*Lv*ement of hemocytes in gut immunity, Dev. Comp. Immunol. 79 (2018) 44–50, https://doi.org/10.1016/j.dci.2017.10.005.

[14] K.J. Livak, T.D. Schmittgen, Analysis of relative gene expression data using realtime quantitative PCR and the 2(-Delta Delta C(T)) method, Methods 25 (2001) 402–408, https://doi.org/10.1006/meth.2001.1262.

[15] R.L. Quispe, E.B. Justino, F.N. Vieira, M.L. Jaramillo, R.D. Rosa, L.M. Perazzolo, Transcriptional profiling of immune-related genes in Pacific white shrimp (*Litopenaeus vannamei*) during ontogenesis, Fish Shellfish Immunol. 58 (2016) 103–107, https://doi.org/10.1016/j.fsi.2016.09.024.

[16] G.M. Matos, P. Schmitt, C. Barreto, N.D. Farias, G. Toledo-Si*Lv*a, F. Guzmán, et al., Massive gene expansion and sequence diversification is associated with diverse tissue distribution, regulation and antimicrobial properties of anti-lipopolysaccharide factors in shrimp, Mar. Drugs 16 (2018) 381, https://doi.org/10.3390/md16100381.

[17] D. Destoumieux-Garzón, D. Saulnier, J. Garnier, C. Jouffrey, P. Bulet, E. Bachère, Crustacean immunity, J. Biol. Chem. 276 (2001) 47070–47077, https://doi.org/10.1074/jbc.M103817200.

[18] V.W. Petit, J.L. Rolland, A. Blond, C. Cazevieille, C. Djediat, J. Peduzzi, et al., A hemocyanin-derived antimicrobial peptide from the penaeid shrimp adopts an alpha-helical structure that specifically permeabilizes fungal membranes, Biochim. Biophys. Acta 1860 (2016) 557–568, https://doi.org/10.1016/j.bbagen.2015.12.010.

[19] B.J. Cuthbertson, E.F. Shepard, R.W. Chapman, P.S. Gross, Diversity of the penaeidin antimicrobial peptides in two shrimp species, Immunogenetics 54 (2002) 442–445, https://doi.org/10.1007/s00251-002-0487-z.

[20] H. Yan, R.E.W. Hancock, Synergistic interactions between mammalian antimicrobial defense peptides, Antimicrob. Agents Chemother. 45 (2001) 1558–1560, https://doi.org/10.1128/AAC.45.5.1558-1560.2001.

[21] P. Schmitt, J. de Lorgeril, Y. Gueguen, D. Destoumieux-Garzón, E. Bachère, Expression, tissue localization and synergy of antimicrobial peptides and proteins in the immune response of the oyster Crassostrea gigas, Dev. Comp. Immunol. 37 (2012) 363–370, https://doi.org/10.1016/j.dci.2012.01.004.

[22] M. Marxer, V. Vollenweider, P. Schmid-Hempel, Insect antimicrobial peptides act synergistically to inhibit a trypanosome parasite, Philos Trans R Soc B Biol Sci 371 (2016) 20150302, https://doi.org/10.1098/rstb.2015.0302.

[23] I.J. McGaw, D.L. Curtis, A review of gastric processing in decapod crustaceans, J. Comp. Physiol. 183 (2013) 443–465, https://doi.org/10.1007/s00360-012-0730-3.

[24] X.W. Wang, J.D. Xu, X.F. Zhao, G.R. Vasta, J.X. Wang, A shrimp C-type lectin inhibits proliferation of the hemolymph microbiota by maintaining the expression of antimicrobial peptides, J. Biol. Chem. 289 (2014) 11779–11790, https://doi.org/10.1074/jbc.M114.552307.

[25] R.D. Rosa, A.A. Vergnes, J. de Lorgeril, P. Gonca*Lv*es, L.M. Perazzolo, L. Sauné, et al., Functional divergence in shrimp anti-lipopolysaccharide factors (ALFs): from recognition of cell wall components to antimicrobial activity, PLoS One 8 (2013) e67937, , https://doi.org/10.1371/journal.pone.0067937.

[26] D. Destoumieux, M. Muñoz, C. Cosseau, J. Rodriguez, P. Bulet, M. Comps, et al., Penaeidins, antimicrobial peptides with chitin-binding activity, are produced and stored in shrimp granulocytes and released after microbial challenge, J. Cell Sci. 113 (2000) 461–469, https://doi.org/10.1016/j.bbagen.2015.12.010.

[27] C. Barreto, J.R. Coelho, J. Yuan, J. Xiang, L.M. Perazzolo, R.D. Rosa, Specific molecular signatures for type II crustins in penaeid shrimp uncovered by the identification of crustin-like antimicrobial peptides in *Litopenaeus vannamei*, Mar. Drugs 16 (2018) 31, https://doi.org/10.3390/md16010031.

TABLE 1

Nucleotide sequences of primers used in this study.

Gene	Forward primer (5′-3′)	Reverse primer (5′-3′)	Amplicon
Primers for molecular cloning and sequencing			
Lvan-STY1	CTGGACGCATCCCTGCTG	TGCGCCTTCGTTCTCTTTATCC	571 bp
Lvan-STY2	GCTGTACTGCTCCTGTGTAG	CTTCGTTCTCGCTTCTTTATCC	589 bp
Primers for tissue distribution analysis (RT-PCR)			
Lvan-Stylicin1	CACAAGAGTGCCCACCGTG	ACATTCGCAGTTATGGTAGCC	125 bp
Lvan-Stylicin2	CACAAGAGTGCCCACCGTG	CACACAGGCTGCCGACATAA	151 bp
*Lv*Actin	TAATCCACATCTGCTGGAAGGTGG	TCACCAACTGGGATGACATGG	846 bp
Primers for absolute and relative quantification analyses (qPCR and RT-qPCR)			
Lvan-Stylicin1	CACAAGAGTGCCCACCGTG	ACATTCGCAGTTATGGTAGCC	125 bp
Lvan-Stylicin2	CACAAGAGTGCCCACCGTG	CACACAGGCTGCCGACATAA	151 bp
*Lv*Actin	CCACGAGACCACCTACAAC	AGCGAGGGCAGTGATTTC	142 bp
*Lv*EF1α	TGGCTGTGAACAAGATGGACA	TTGTAGCCCACCTTCTTGACG	103 bp
*Lv*L40	GAGAATGTGAAGGCCAAGATC	TCAGAGAGAGTGCGACCATC	104 bp
*Lv*RpS3A	GGCTTGCTATGGTGTGCTCC	TCATGCTCTTGGCTCGCTG	101 bp
*Lv*RpS6	AGCAGATACCCTTGGTGAAG	GATGCAACCACGGACTGAC	193 bp

FIGURE 1

(A) Nucleotide and deduced amino acid sequences (one letter code) of *Lvan*-Stylicin1 (GenBank: MH108957) and *Lvan*-Stylicin2 (GenBank: MH108958). The predicted signal peptides are in bold and underlined. Asterisks (*) mark the stop codon. (B) Amino acid sequence alignments of stylicins from penaeid shrimp species from the genus *Litopenaeus* (*Lv*an: *L. vannamei* and *Lsty*: *L. stylirostris*). Identical amino acid residues are highlighted in black while specific amino acid residues found in Stylicin1 and Stylicin2 peptides are highlighted in blue and yellow, respectively. Triangles (▼) indicate the 13 conserved cysteine residues. GenBank accession numbers are indicated in brackets. The sequences of the *Vibrio penaeicida*-induced cysteine and proline-rich peptides (*Lv*VICP1 and *Lv*VICP2) were obtained from Ref. [9]. (For interpretation of the references to colour in this figure legend, the reader is referred to the Web version of this article.)

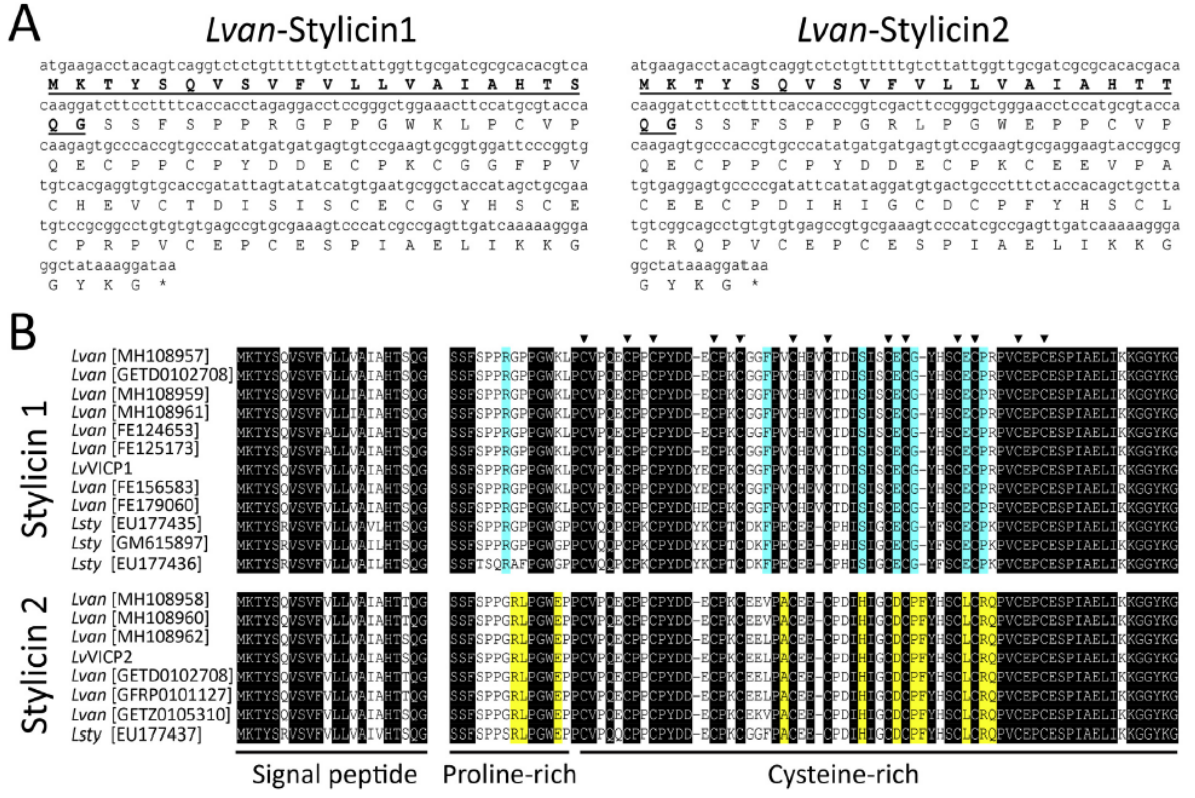

FIGURE 2

(A) Not-to-scale schematic representation of stylicin genes from *Litopenaeus vannamei* (*Lvan-STY1* and *Lvan-STY2*). Boxes represent the exons and the line between boxes represents the intron. Numbers indicate the length of exons and introns in base pairs. (B) Estimation of the copy number of *Lvan*-STY genes in five individual shrimp. The absolute quantification was assessed by qPCR using a standard curve derived from 10-fold dilution series of plasmids containing each target gene. Results are presented as the ratio of the abundance of *Lvan-STY2* gene copies per ng of gDNA to that of *Lvan-STY1*. (C) Structural organization and phylogenetic relationship of STY genes from penaeid shrimp: *Litopenaeus vannamei* (*Lvan-STY1*: MH108959 and MH108961; *Lvan-STY2*: MH108960 and MH108962), *Litopenaeus stylirostris* (*Lsty-STY1*: EU177436; *Lsty-STY2*: EU177437), Penaeus monodon (*Pmon-STY*: NIUS012084699) and *Marsupenaeus japonicus* (*Mjap*-STY: NIUR011088360).

The cladogram at the left of the figure indicates the phylogenetic relationship of STY genes. Pink and yellow boxes indicate the position of the signal peptides and the mature stylicins in the exons, respectively, while the black lines indicate the introns. (For interpretation of the references to colour in this figure legend, the reader is referred to the Web version of this article.)

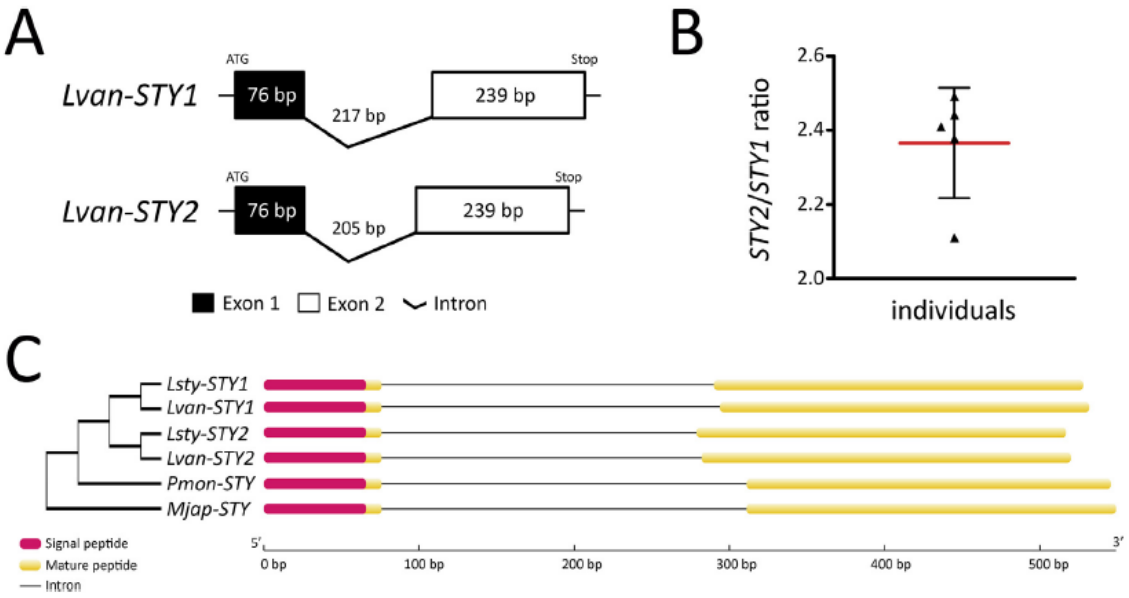

FIGURE 3

(A) Amino acid sequence alignments of mature peptides of stylicins. Identical amino acid residues are highlighted in black. Triangles (▼) indicate the 13 conserved cysteine residues. GenBank accession numbers are indicated in brackets. (B) Phylogenetic analysis of stylicins from penaeid shrimp. The tree was constructed using the Maximum Likelihood method with bootstrap values calculated from 1000 trees. Sequences included in analyses were the following: *Litopenaeus vannamei* (*Lvan*-Stylicin1: MH108957, MH108959, MH108961, FE179060, FE156583, FE124653, FE125173, GETD01027084 and *Lv*VICP1; *Lvan*-Stylicin2: MH108958, MH108960, MH108962, GETD01027083, GFRP01011277, GETZ01053100 and *Lv*VICP2), *Litopenaeus stylirostris* (*Lsty*-Stylicin1: EU177435, EU177436 and GM615897; *Lsty*-Stylicin2: EU177437), Fenneropenaeus penicillatus (Fpen-Stylicin: GFRT01005742), Penaeus monodon (*Pmon-STY*licin: JZ892895, DW678047, DW678039, DT366712, DW042940, GW996588, GEEP01015864, GEME01013089 and NIUS012084699) and *Marsupenaeus japonicus* (*Mjap*-Stylicin: KR063277 and NIUR011088360).

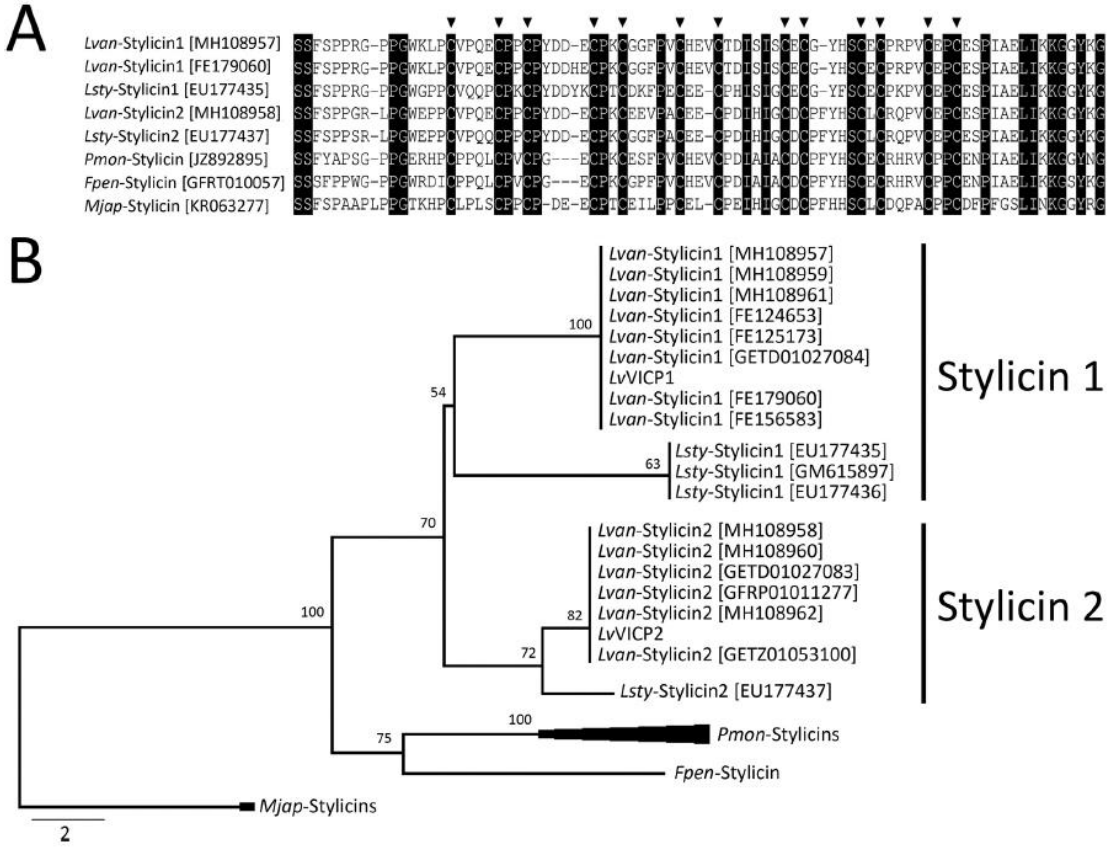

FIGURE 4

Gene expression distribution of *Litopenaeus vannamei* stylicins (*Lvan*-Stylicin1 and *Lvan*-Stylicin2) in different tissues from naïve (N) and *Vibrio*-stimulated (S) shrimp. Gene expression analysis was performed by semiquantitative RT-PCR using the β-actin gene (*Lv*Actin) as an endogenous expression control. The figure (not-to-scale) shown at the top of the figure indicates the anatomic location of shrimp tissues: foregut (FG), hepatopancreas (HP), midgut (MG), hindgut (HG), circulating hemocytes (HE), muscle (ML), gills (GL) and nerve cord (NC).

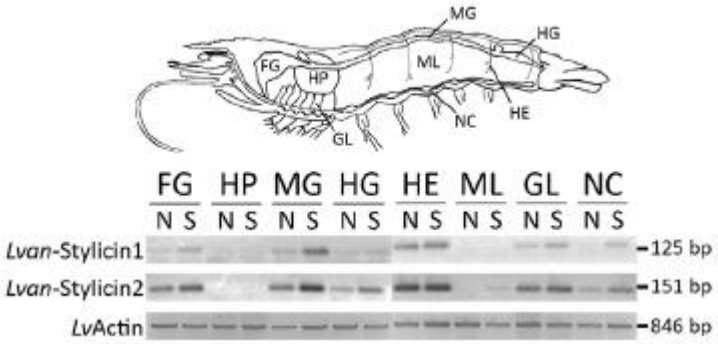

FIGURE 5

(A) Immunodetection of *Lvan*-Stylicin peptides in shrimp tissues by immunohistochemistry. Stylicin immune reactivity was observed in hemocytes infiltrating the connective tissue (arrows) and in the columnar epithelium of the midgut. The figure (not-to-scale) shown at the top panel indicates the anatomic location of shrimp tissues: anterior midgut caecum (AMC), midgut (MG) and hepatopancreas (HP). Scale bars=100 µm. (B) A magnification of the anterior midgut caecum. The arrows indicate stylicin-expressing hemocytes infiltrating connective tissues. Negative controls consisted in replacing primary antibodies with pre-immune mouse serum (bottom panel). Scale bars=100 µm. (C) Scanning confocal microscopy images of the immunodetection (whole mount immunofluorescence staining) of *Lvan*- Stylicin peptides present in granules located at the apical region of the midgut columnar epithelial cells. (D) Nuclei of the midgut columnar epithelial cells stained with DAPI. (E) Merged images of the stylicin-containing granules (green) and the nuclei (blue) of the midgut columnar epithelial cells. Scale bars=20 µm. (For interpretation of the references to colour in this figure legend, the reader is referred to the Web version of this article.)

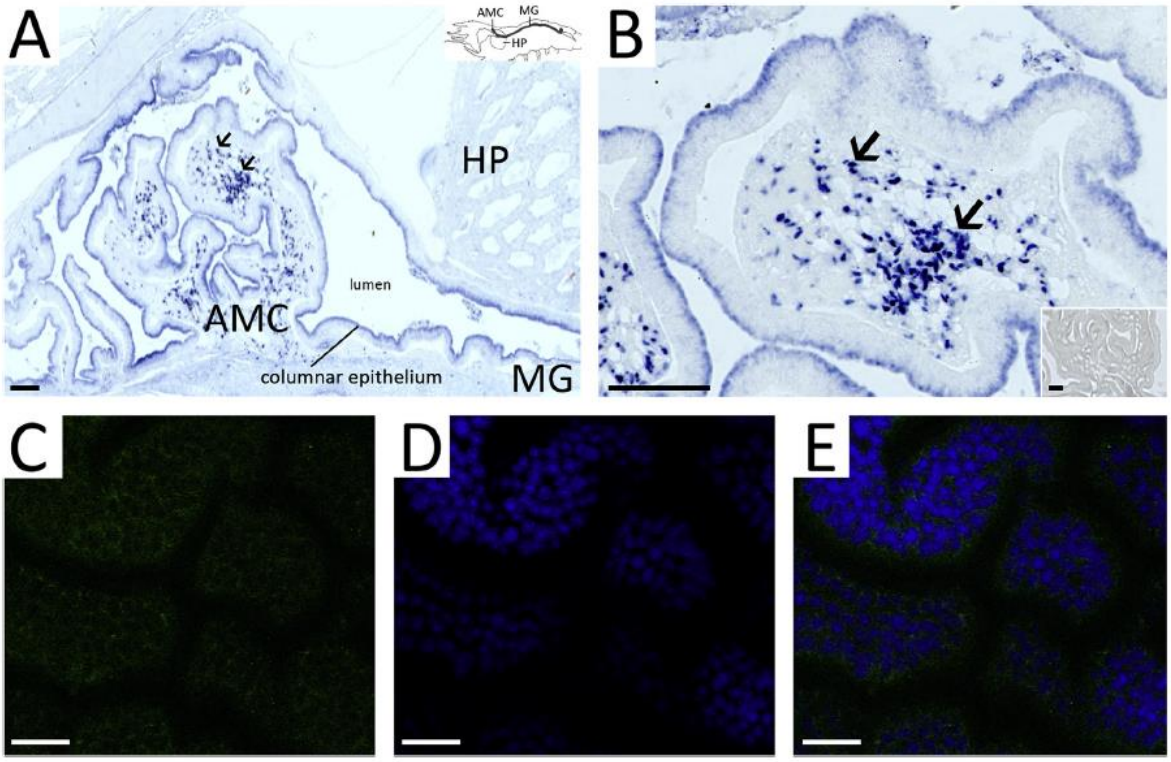

FIGURE 6

(A) Quantitative comparison of the relative abundance of *Lvan*-Stylicin1 (white bars) and *Lvan*-Stylicin2 (black bars) transcripts in circulating hemocytes (HE) and midgut (MG). Results are presented as mean ± standard deviation of relative expressions (three biological replicates) and statistical differences are indicated by asterisks (*) (Student's t-test, $P < 0.05$). (B) Transcript abundance of *Lvan*-Stylicins in five individual shrimp. The absolute quantification was assessed by qPCR using a standard curve derived from 10-fold dilution series of plasmids containing each target gene. Results are presented as the ratio of the abundance of *Lvan*-Stylicin2 transcripts per ng of total RNA to that of *Lvan*- Stylicin1. The β-actin gene (*Lv*Actin) was used as endogenous expression control for each individual shrimp (lower panel).

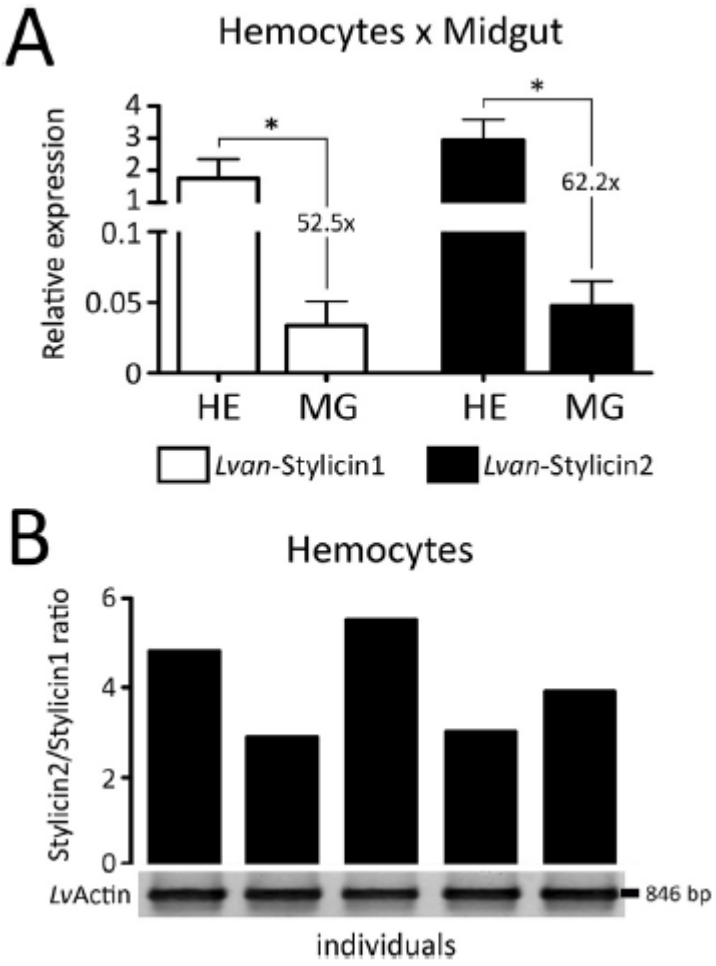

FIGURE 7

Relative gene expression profile of *Lvan*-Stylicin1 (white bars) and *Lvan*-Stylicin2 (black bars) in circulating hemocytes and midgut of shrimp at 48 h after experimental infections with the Gram-negative *Vibrio harveyi* ATCC 14126 (6×107 CFU/animal) or the White spot syndrome virus (WSSV: 3×102 viral particles/ animal). Results are presented as mean ± standard deviation of relative expressions (three biological replicates) and statistical differences are indicated by asterisks (*) (one-way ANOVA/Tukey, P < 0.05). W-free: tissue homogenate inoculum prepared from WSSV-free shrimp.

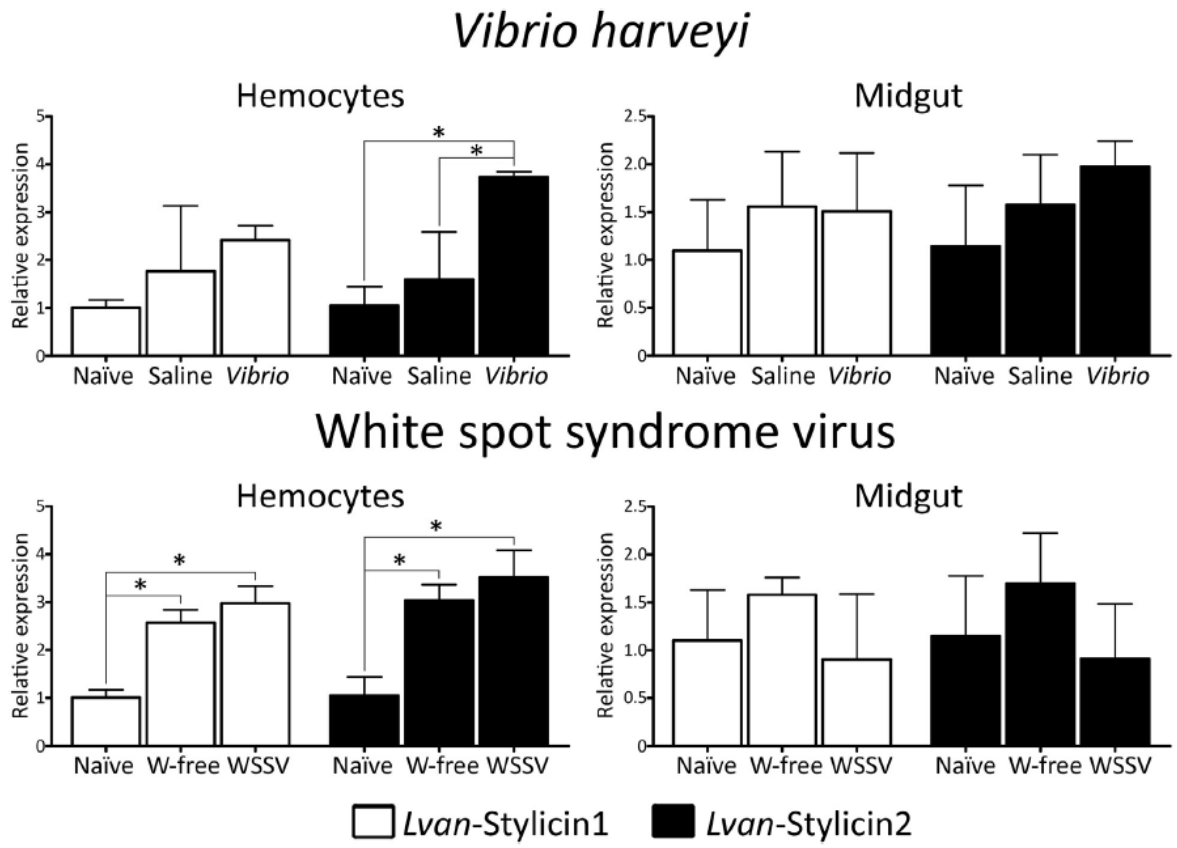

FIGURE 8

Relative gene expression profile of *Lvan*-Stylicin1 and *Lvan*-Stylicin2 in three portions of shrimp midgut (anterior, middle and posterior) at 21 h after the oral administration of 7.5×105 CFU/animal of live V. *harveyi* ATCC 14126. Results are presented as mean ± standard deviation of relative expressions (three biological replicates) and statistical differences are indicated by asterisks (*) (Student's t-test, P < 0.05). The figure (not-to-scale) shown at the top of the figure indicates the anatomic location of the three midgut portions from naïve (white bars) and *Vibrio*-challenged (black bars) shrimp.

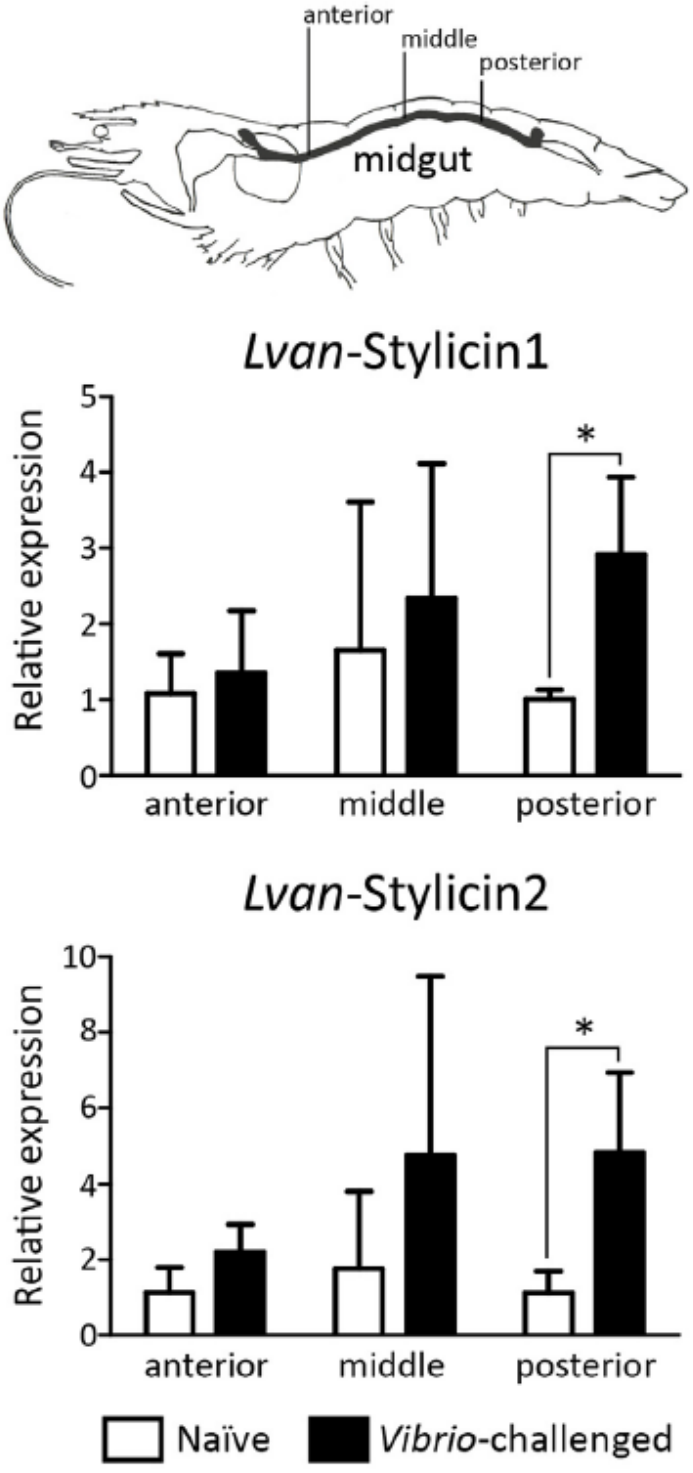

FIGURE 9

Gene expression profile of *Litopenaeus vannamei* stylicins during shrimp development. EI: fertilized eggs at 0–4 h post-spawning; EII: fertilized eggs at 7–11 h post-spawning; NI: nauplius I; NV: nauplius V; ZI: protozoea I; ZIII: protozoea III; MI: mysis I; MIII: mysis III; PL2: postlarva 2; PL9: postlarva 9; PL17: postlarva 17. The red dotted line indicates the basal expression level in hemocytes from juvenile shrimp while the solid blue underline highlights the stages at which the gene expression was detected (valid dissociation curve profile) but not quantified (Cq values higher than the limit of quantification). Results are presented as mean ± standard deviation (three biological replicates). Different letters indicate significant differences among the development stages while asterisks (*) shows significant differences between each developmental stage and hemocytes from juveniles (one-way ANOVA/Tukey, $P < 0.05$). (For interpretation of the references to colour in this figure legend, the reader is referred to the Web version of this article.)